Fibers and Polymers 2017, Vol.18, No.12, 2469-2475
DOI 10.1007/s12221-017-7560-6

ISSN 1229-9197 (print version)
ISSN 1875-0052 (electronic version)

Investigation on Laser Engraving Based Application of Silica Aerogel into Nonwovens

Xiaoman Xiong*, Tao Yang, Rajesh Mishra, Jakub Wiener, and Jiří Militký

Department of Material Engineering, Faculty of Textile Engineering, Technical University of Liberec, Liberec 46117, Czech Republic

(Received June 29, 2017; Revised October 2, 2017; Accepted October 22, 2017)

Abstract: In this work, a new approach to apply silica aerogel into nonwoven textiles by using laser engraving and laminating technique was proposed. Thermal performance of the prepared composites were characterized in terms of infrared thermal images, maximum heat flux and heat retention ability. Results showed that in comparison to regular composites the air pockets lead to 0.5 °C lower temperature on the fabric surface, and the aerogel-encapsulated structure results in a decrease of 1.04-1.47 °C in the fabric temperature. It was also noticed the aerogel-encapsulated composites have slightly lower q_{max} value and a thermal feeling, however, samples with air pockets showed increased value in q_{max}, and the increasing rate was strongly related to the composites thickness. Composites with air pockets exhibited better ability to retain heat, the highest heat retention ability was observed from composites with aerogel-encapsulated structure.

Keywords: Silica aerogel, Nonwoven fabrics, Laser engraving, Maximum heat flux, Heat retention ability

Introduction

Silica aerogel is cross-linked structure of silica dioxide with a large number of air-filled nano-scale pores. Silica aerogels are synthesized via a sol-gel process followed by supercritical drying of the wet gel in an autoclave. This traditionally practiced production process and normally used expensive raw materials prevented a production in an industrial scale. Recently, the successful and cost effective production of silica aerogels by use of inexpensive precursors and ambient pressure drying method has been achieved [1], which raises the possibility of continuous production with lower operating costs for industrial application.

Due to its extraordinary small pore sizes and high porosity, silica aerogel exhibits the most fascinating properties such as low thermal conductivity (0.015 W/mK), low bulk density (0.1 g/cm^3), optical transparency in the visible spectrum (99 %), high specific surface area (1000 m^2/g), low dielectric constant (1.0-2.0), low refractive index (1.05), low sound velocity (100 m/s) and hydrophobicity [2-4]. Among these characteristics, the most attractive one is its extremely low thermal conductivity. Nowadays, silica aerogel has well been acknowledged as one of the most attracting thermal insulating materials for applications in heat-protective clothing, automotive industry as well as in building and construction products. The excellent thermal insulation properties of aerogels are determined by their nanoporous structure which can provide a barrier to the collision of gas molecules. It is well known that heat transfers in a still gas by means of molecular collisions, faster (hot) moving molecules collide with slower (cold) moving molecules and pass on some of their heat energy. In an aerogel, since the mean free path of gas molecules, the average distance which a gas molecule travels before it collides with another molecule, is smaller than that in free space, the motion of the gas molecules in the aerogel is retarded, which can act as a barrier to prevent the collision process. Thus, the molecules will not collide with each other but rather collide with the barrier from which they rebound and therefore, retain their heat energy and reduce heat transfer [5].

In general, aerogel can be used as loose bulk material for thermal insulation, but for the majority of applications a bound form such as aerogel containing sheet is required. For this purpose lightweight textile fabric is usually used and proper binding material can be considered. Based on this consideration, a lot of effort has been made to explore the combination of silica aerogel with textile fabrics as thermal insulator. Aerogel particles have been embedded into the thermal barrier layer of firefighters' protective clothing (FPC), the backside temperature of the FPC samples with aerogel was about 100 °C lower than that of samples without aerogel when exposed to radiant heat [6]. A study on incorporated super hydrophobic silica aerogel nanoparticles in 65/35 wool-Aramid blended fabrics indicated that only 2 % coating of aerogel nanoparticle increases thermal resistance by up to 68.64 % [7]. Some researcher applied silica aerogel on the surface of cotton woven fabrics by coating and found that pique showed the lowest values in thermal resistance and satin showed the highest values while plain weave lied in between. Furthermore, it was also reported that the thermal properties of treated high-density cotton plain weave fabric were strongly influenced by finishing agent concentration [8]. With respect to aerogel-based nonwoven fabrics, the fibrous structure density and the aerogel present in the polyester/polyethylene fibrous nonwovens with silica aerogel impregnation were believed

*Corresponding author: xiaoman.xiong@tul.cz

to have significant effect on thermal properties of the overall structures [9]. Meanwhile, thermal insulation of aerogel-treated nonwoven was observed to strongly dependent on the weight and compressional properties of the fabric [10]. The modeling and simulation of heat transfer for aerogel-treated nonwoven fabric indicated that thermal behavior of the fabric improved when treated with aerogel [11]. These studies all confirmed that the present aerogel in textile structure can significantly improve the thermal performance, however, the application of aerogel granules has so far been limited in a few methods such as coating, padding and impregnating, with the assistant of additive agent. Since aerogel granules are exposed or filled into the void space in textile structure, and the porous space of the loose textile structure is partly filled by additive agent, these will cause negative effect on the final thermal performance since the porous space is essential and useful to entrap air pockets to enhance thermal insulation properties. Meanwhile, the nanopores of aerogel granules are filled or covered by binding materials, which would reduce their superiority of high thermal insulation ability [12]. Thus, to make the final insulating material more effective, use less or even no binder to combine silica aerogel with high porous textiles could be a better consideration to develop aerogel-based nonwoven thermal insulators.

University of Leeds developed Hydrospace™ fabric from a carded and cross-laid web. This fabric enables the formation of moulded voids within the cross-section of hydroentangled fabrics and simultaneous filling of these voids with loose aerogel particles composed of amorphous silica [5]. The size, shape and frequency of the filled voids can be varied according to the dimensions of the encapsulated materials. However, the details of fabrication method was not given.

In this work, a new approach to apply silica aerogel into textile for thermal insulation was proposed. To take benefit of air trapping potential in porous materials, high porous nonwoven fabrics were selected as support layers to produce perforations by laser engraving, a thin cloth layer was bonded on the bottom, aerogel granules were subsequently injected into these holes followed by the laminating of the same cloth layer on the surface to prevent against aerogel loss. Since the entire process doesn't involve any binder to bond aerogel particles, the final obtained composites would have markedly enhanced thermal insulation ability. Meanwhile, this new technique used to combine aerogel with textiles enables the final products to be more flexible, our materials will be more advantageous for potential application in clothing field.

Thermal performance of prepared composites were measured and analyzed in terms of infrared thermal images, heat retention ability and thermal contact property. The findings in this work could contribute to new developments in flexible aerogel-based high-performance composites for clothing application.

Experimental

Materials

The aerogel-containing fabric system was designed with a composite structure. This composite has three layers: a support layer, a base layer on the bottom and a face layer on the surface. In this work, three types of nonwoven fabrics prepared at Technical University of Liberec (TUL), Czech Republic, by using a vibrating perpendicular lapper, were selected as support layer to hold silica aerogels. The nonwoven samples were made by 70 % PET and 30 % bi-component PET fibers, the fiber specifications are listed in Table 1. The sheath part of bi-component fibers is low-melting polyethylene terephthalate (PET) with melting temperature around 120 ^{o}C, and the core part is polyethylene terephthalate (PET) with melting temperature 160-180 ^{o}C. The thermal conductivity values of PET and Bi-component PET are between 0.15 W/m K and 0.24 W/m K.

The vibrating perpendicular lapper used to fabricate struto nonwovens is illustrated in Figure 1. The carded web is fed onto the conveyor belt and a reciprocating forming comb pulls the carded web toward the hold back roller to form a fold. The fold is pulled off the comb by a system of needles placed on a reciprocating compressing bar and pushed to the fiber layer, which is created and moved between the conveyor belt and a wire grid [13]. The fiber layer is bonded by melting bonding fibers present in the fiber blend when it

Table 1. Specifications of polyester fibers used to fabricate nonwovens

Fiber type	Diameter (μm)	Fineness (dtex)	Fiber length (mm)	Ratio of core and sheath
PET	26.91	6.70	57.00	-
Biocomponent PET	14.58	2.20	38.00	3:1

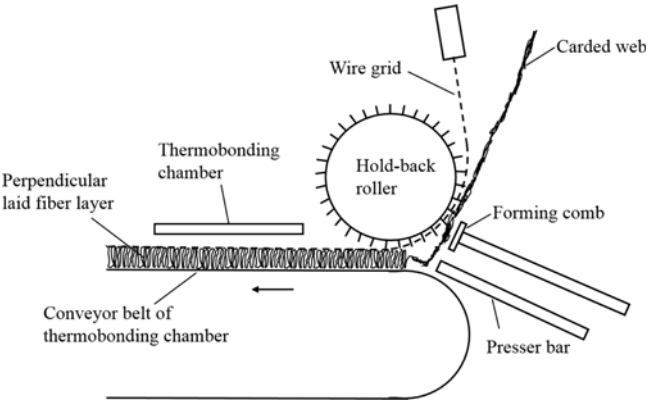

Figure 1. Vibrating perpendicular lapper used to fabricate struto nonwovens.

Table 2. Characterizations of prepared nonwovens

Sample code	Material	Porosity (%)	Thickness (mm)	GSM (g/m^2)
P	High-loft nonwoven	96.69	12.42	317.51
M	High-loft nonwoven	97.93	9.68	259.28
N	High-loft nonwoven	99.19	12.05	198.64

Table 3. Specifications of aerogel granules

Properties	Value range
Particle size (mm)	0.1-0.7
Pore diameter (nm)	~20
Particle density (kg/m^3)	About 120
Surface chemistry	Fully hydrophobic
Thermal conductivity (W/m·K)	0.012 (at 25 °C)

passes through the thermo-bonding chamber.

The characteristics of the obtained nonwoven specimens are listed in Table 2. Fabric weights per unit area were determined according to ASTM D1059 standard using electronic weighing scales, fabric thicknesses were measured according to ASTM D1777-96 standard with the SDL digital thickness gauge at a pressure of 100 Pa, porosity values were determined according to ASTM C 830-00 Standard Test Methods for Apparent Porosity, Liquid Absorption, Apparent Specific Gravity.

Silica aerogel granules were purchased from Cabot aerogel Corp, the specifications of the aerogel granule are shown in Table 3. A spun-melt PET nonwoven fabric with thickness 0.25 mm and GSM 25 g/m^2 was used as cover layer (S) to laminate onto both sides of the support layers. In order to bond the cover fabric S with support layer and maintain the flexibility of the multilayer composite, a commercial available extra soft textile adhesive film with thickness 0.10 mm, was used for laminating process. This adhesive film is made by applying acrylic adhesives to polyethylene film.

Laser Treatment of Support Layer

In order to produce perforations on the nonwoven fabrics to encapsulate silica aerogels, the support layers (P, M and N) were treated by a commercial pulsed CO_2 laser system GFK Marcatex FLEXI-150 to remove certain materials as the laser beam vaporizes the surface [14]. This CO_2 laser machine consists of CO_2 laser, computer laser treatment software, automatic control and laser mechanics. The laser treatment can make design on fabrics by scanning the design by line with the laser, according to the resolution dot of designed graphic images. The laser head moves back and forth to engrave a series of dots in one line at a time. While it moves line by line, the dot pattern will form the designed image by laser engraving on fabrics [15].

Before the laser treatment, the holes pattern file was designed in grey scale by Photoshop CS4 graphic design software as shown in Figure 2.

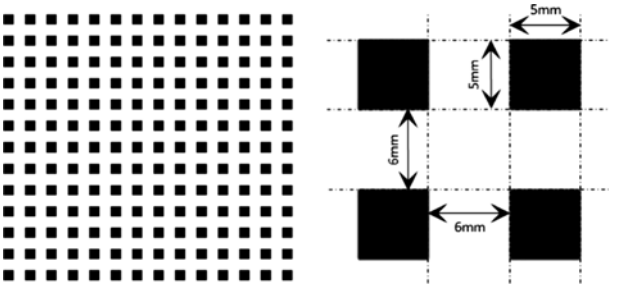

Figure 2. Designed holes pattern.

The generated wavelength of laser beam was set at 10.6 μm and the input voltage was 100 V. Nonwoven samples were placed in the laser treatment cabinet for testing with different parameters such as duty circle, pixel time and resolution, followed by the laser engraving on nonwovens with optimized parameters. The duty cycle is synonymous with the power applied and represents the ratio of the laser time on (pulse width) and laser time off. Its maximum value is 50 % for the equipment used. The pixel time is time in microseconds used to mark each pixel of the image [16]. Therefore, by adjusting duty cycle and pixel time it is possible to search out the best experimental conditions with this specific equipment. The specifications of optimized parameters are listed in Table 4. P', M' and N' refer to laser-engraved support layers, corresponding to nonwoven materials P, M and N respectively.

Since the obtained holes dimension is strongly dependent on the structural parameters and physical properties of the

Table 4. Specifications of parameters for laser treatment

Parameter	P'	M'	N'
Duty circle (%)	50	50	45
Pixel time (μs)	100	50	50
Resolution (dpi)	96	96	96

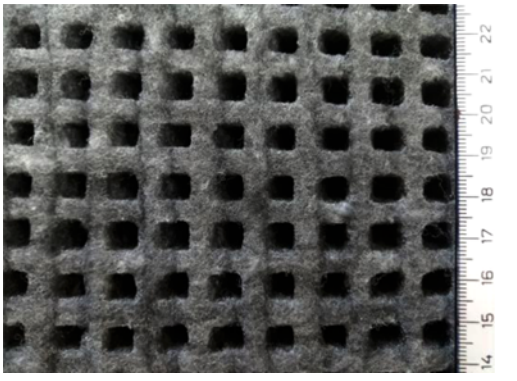

Figure 3. Typical image of laser-engraved middle layer.

support layers, in order to achieve the designed holes size for different support layers, the duty circle and pixel time required for laser treatment varies with the fabric thickness and GSM. The typical image of laser engraved sample is shown in Figure 3.

Laminating

Conventionally, laminating can be used to combine two fabrics by applying adhesive or using heat and pressure. A laminated technical textile normally consists of two or more textile layers, bonded closely together by means of an added adhesive or the adhesive properties of the component layers [17].

In this work, the covering fabric was laminated onto the struto nonwovens using textile adhesive film. A piece of adhesive film was inserted between the covering fabric (S) and a laser-treated support layer, proper pressure was applied to bring sufficient adhesive effect between the support layer and covering fabric. The obtained fabrics was then turned over, aerogel granules were uniformly injected into these laser-engraved holes using a syringe barrel, the amount of aerogel in each hole was kept the same by controlling the plunger. Another covering fabric was subsequently combined with the composites to form a closed fabric system. The fabrication process was illustrated in Figure 4.

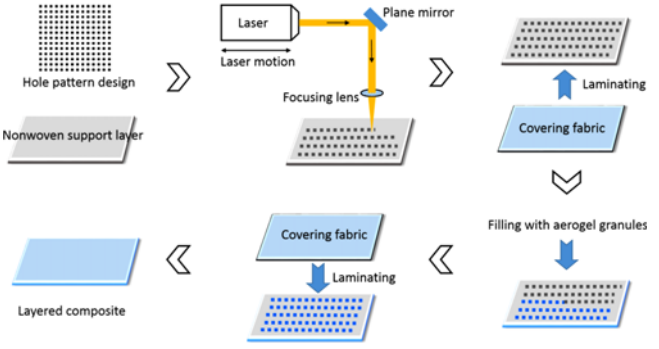

Figure 4. Fabrication process of aerogel-encapsulated composite.

Table 5. Characterizations of multi-layered composites

Sample code	Composite structure	Aerogel content (g/m^2)	Thickness (mm)	GSM (g/m^2)
A1	SPS	-	12.80	420.32
A2	SP'S	-	12.92	386.58
A3	SP"S	31.89	12.88	415.25
B1	SMS	-	9.88	363.41
B2	SM'S	-	10.11	344.75
B3	SM"S	42.35	9.93	391.36
C1	SNS	-	12.50	399.57
C2	SN'S	-	12.64	279.38
C3	SN"S	34.68	12.64	322.65

The resultant composites were multi-layered materials, with aerogel-encapsulated nonwovens (P", M" and N") as middle layers. Different cases of middle layers including untreated nonwovens (P, M and N) and nonwoven with air pockets (P', M' and N') were prepared as control samples. The details of the prepared composites are listed in Table 5.

Testing Methods

Thermography Images

Test was carried out in a thermal chamber. A guard hot plate with constant temperature 33 °C was installed in this chamber to provide uniform thermal radiation, a thermal camera was fixed in the air space with a distance of 40 cm from the hot plate. When the specimen was placed on the hot plate, pictures were taken every 5 second up to when the heat transfer reaches steady state. The room temperature was kept at 23±2 °C. The specimen size used for measurements was 20 cm×20 cm, three tests were carried out for each sample. The temperature of the surface was calculated using Avio Thermography Studio 2007 software.

KES-FT-II Thermolab Tester

KES-FT-II Thermolab Tester was employed to determine maximum heat flux q_{max} and heat retention ability of prepared samples. This device contains Measuring box T, Measuring box BT, Larger measuring box BT, Cooling box and Wind column, which are respectively used to measure warm or cold feeling, thermal conductivity, heat loss to determine heat retention ability, maintain a constant temperature and inlet constant airflow [18].

Maximum heat flux q_{max}, describing the thermal contact properties of textile fabrics, is evaluated by measuring the peak value of the transferred heat from the heated plate to the fabric sample. Measuring box T is deposited on the preheated BT plate to be heated, the temperature of this BT plate is kept at 33 °C to simulate a human skin condition. The fabric to be measured is placed on the cooling box which is maintained at constant temperature 23 °C. When the measuring box T reaches a desired temperature 33 °C, it is quickly shifted onto the fabric surface. The value of q_{max} [W/cm^2] is reached for 0.2 seconds from the moment of contact. A higher q_{max} value indicates more rapid movement of heat from the body to the fabric surface and a cooler feeling fabric.

Heat retention ability, defined as the percentage reduction in heat loss from a hot surface maintained at a given temperature, is measured by using Larger BT box and wind column. The BT plate is heated to a temperature of 33 °C, a constant air flow rate of 0.3 m/s with a constant air temperature of 23±2 °C is supplied from the wind column. Constant air flow can be achieved by adjusting the fan speed. Loss of heat flow in both conditions, without fabric on BT plate and with fabric on BT plate, are measured. From the obtained values of the heat flow loss, the heat retention ability α can be calculated according to the formula:

$$\alpha = \frac{W_0 - W}{W_0} \times 100$$

where W is the amount of heat release (W) with a sample placed on heat plate, W_0 (W) is the amount of heat release without fabric.

Results and Discussion

Infrared Thermal Images

Thermal images are actually visual displays of the amount of infrared energy emitted, transmitted, and reflected by an object. The amount of radiation emitted by the heat plate through the fabric was detected, therefore the thermography allows to see temperature variations. Figure 5 shows the infrared thermography images of prepared composites. For each group, the detected temperatures of samples with air pockets were observed to be lower than that from regular samples, and the lowest values were from aerogel-encapsulated composites, indicating that the encapsulated aerogel can significantly enhance thermal insulation ability.

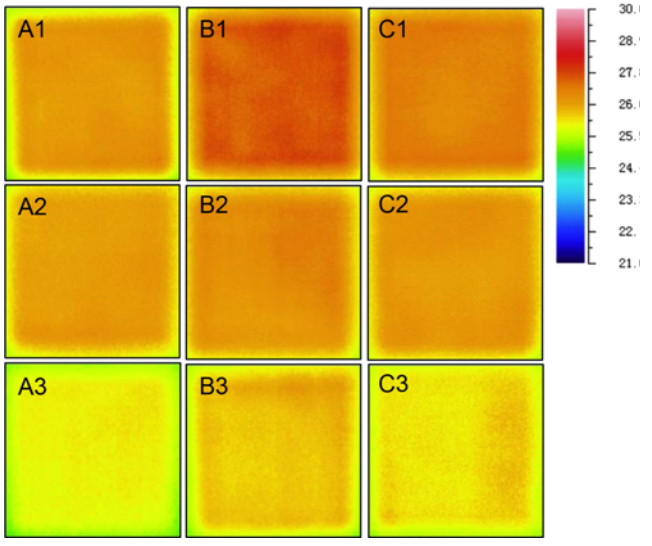

Figure 5. Infrared thermography images.

Table 6. Thermal performance of different composites

Sample code	Detected temperature (°C)		q_{max} (W/cm^2)		Heat retention ability (%)	
	Mean	SD	Mean	SD	Mean	SD
A1	27.30	0.20	28.5	2.72	70.44	1.99
A2	26.83	0.15	37.9	2.28	72.66	2.46
A3	25.83	0.15	26.6	2.22	76.37	1.78
B1	27.57	0.12	33.8	1.87	68.85	1.91
B2	27.00	0.08	34.6	1.84	71.36	1.46
B3	26.53	0.15	30.4	2.07	75.41	1.68
C1	27.47	0.15	32.2	2.25	69.98	2.62
C2	27.00	0.10	41.8	2.17	72.56	2.34
C3	26.20	0.10	30.6	2.17	76.95	1.47

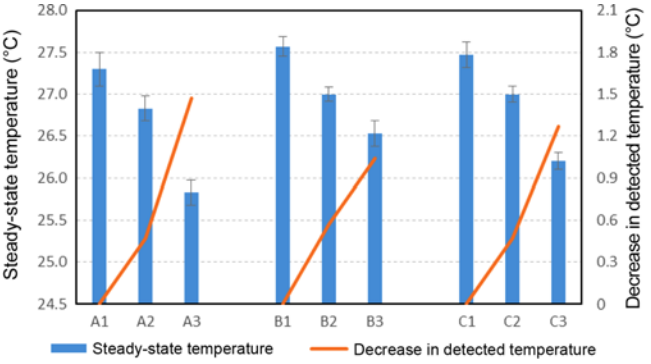

Figure 6. Temperature of composite surface under steady state.

The detected temperature of all the prepared composites are shown in Table 6 and Figure 6. The temperature from regular samples A1, B1 and C1 were 27.30 °C, 27.57 °C and 27.47 °C respectively, whereas for samples with air-filled holes (A2, B2 and C2) were only 26.83 °C, 27.00 °C, and 27.00 °C while these values for aerogel-encapsulated samples (A3, B3 and C3) were 25.83 °C, 26.53 °C and 26.20 °C respectively. It is clear that the air pockets gave rise to a decrease of around 0.5 °C in fabric temperature as seen in Figure 6, a temperature gap of 1.04 °C to 1.47 °C was also observed between aerogel-encapsulated samples and regular samples under a temperature difference 10 °C between hot plate and environment. Normally, this temperature gap will be enlarged under greater temperature difference condition.

Maximum Heat Flux

Maximum heat flux q_{max} is the transitional thermal exchange at the time of contact between skin and the fabric. The warm/cool feeling, as the result of the rapid transfer of heat flux from the skin to the fabric surface immediately after the fabric is placed in contact with the skin, is a transient heat conduction phenomenon. This sensation that arises from thermal contact property is essential for engineering fabrics to provide clothing comfort.

The measured values of q_{max} are presented in Table 6 and Figure 7. It is clear that the q_{max} value of aerogel-encapsulated samples was noticed to be slightly lower than regular composites, indicating a slower heat transfer and a thermal feeling. The warm/cool sensation, resulted as heat flow from the skin to a fabric, is strongly related to the surface condition especially the surface contour of the fabric [19]. Since the contact between skin simulating heat source and fabric surface is reduced by an irregular surface contour of the aerogel-encapsulated composites, it will result in the lowering of q_{max} value and warmer feeling.

The highest q_{max} values were observed from samples with air pockets, revealing more heat flux transferred and a cooler

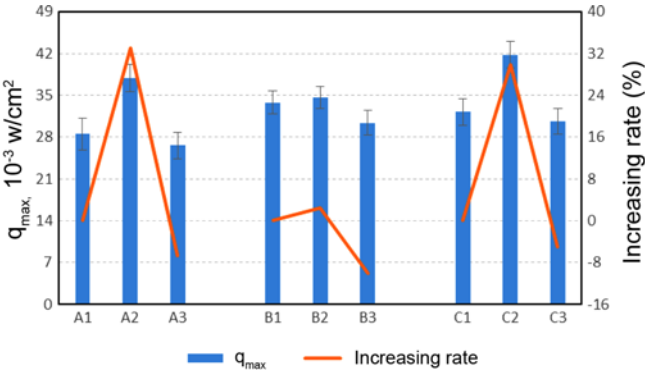

Figure 7. Measured q_{max} values.

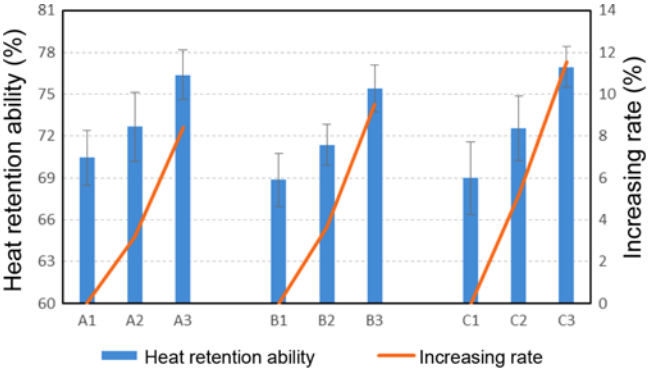

Figure 8. Heat retention ability of different composites.

sensation. The reason could be that due to the existence of many air pockets in their structure these samples have more flattened surface when the measuring T box was placed onto fabric surface during the cool/warm feeling testing, leading to a smoother surface. A smoother surface profile leads to an increased thermal contact between heat source and fabric [20]. Therefore, more heat flux transferred by heat conduction.

According to Table 5 and Figure 7, it is also found that air-filled samples with higher thickness (A2 and C2) had higher q_{max} values, with an increasing of about 32 % compared to regular samples (A1 and C1). The thinnest sample B2, with a thickness of 10.11 mm, showed the lowest q_{max} value among the three samples with air pockets. Meanwhile, its increasing rate in q_{max} was less than 4 %, much lower than those of sample A2 and C2.

Heat Retention Ability

Heat retention ability of textile fabric depends upon the thermal insulation performance of the fibrous assembly and the thermal emission characteristics of the surface fabric. Since nonwoven fabrics possess a large amount of void space, their thermal insulation performance are determined by the air trapped in the inter-fiber spaces. Thereby, the ability of heat retention is also strongly influenced by the air voids in the fabric structure.

The heat retention ability of different composites are illustrated in Figure 8. It is apparent that samples with air-filled voids (A2, B2 and C2) had better ability to retain heat compared to regular samples A1, B1 and C1. This is because the large voids formed by laser treatment can enlarge the amount of still air in the composites structure, meanwhile, the amount of solid fibers is reduced, causing less heat transfer between solid fibers and through the fabrics.

The highest heat retention ability were observed from composites with aerogel-encapsulated structure (A3, B3 and C3). Since the heat transfer in aerogel is effected through its solid-state component, the air occupying the pores is a bad heat conductor. Moreover, due to the microporous aerogel structure and its extremely small pore size which determines the small path lengths of the molecules, the gas conductivity becomes substantially lower than that for a free gas [21]. Evacuating air from the aerogel pores additionally reduces its heat transfer. As a result, aerogel-encapsulated samples exhibited enhanced heat retention ability. The increasing of heat retention ranged from 3.15 % to 5.19 % for composites with air pockets, and this value for aerogel-encapsulated composites lied between 8.42 % and 11.55 %.

Conclusion

Three types of struto nonwoven fabrics developed by vibrating perpendicular lapper were selected to produce perforations by means of laser engraving treatment, the obtained perforated nonwovens were combined with thin fabric layer on both sides by lamination method, silica aerogel was injected into these holes before the closed systems were prepared. Thermal performance of the prepared composites was characterized. Infrared thermography data were collected by IT Flex Cam Thermal Imager, thermal contact property and heat retention ability were determined by KES-FT-II Thermolab Tester.

Results showed that in comparison to regular composites the air pockets lead to 0.5 ^{o}C lower temperature on the fabric surface, and the aerogel-encapsulated structure results in a decrease of 1.04-1.47 ^{o}C in the fabric temperature. It was also noticed the aerogel-encapsulated composites have slightly lower q_{max} value and a thermal feeling, the air-filled samples with higher thickness have higher q_{max} values, with an increase of about 32 % compared to regular samples. Composites with air pockets showed better ability to retain heat, the highest heat retention ability were observed from composites with aerogel-encapsulated structure.

In order to further explore the potential of using this novel technique to fabricate flexible aerogel-based materials for clothing application, more work is required to study the thermo-physiological characteristics of the final products.

Acknowledgement

This work was supported by the research project of Student Grant Competition of Technical University of Liberec no. 21195/2017 granted by Ministry of Education Youth and Sports of Czech Republic.

References

1. H. Bargozin, L. Amirkhani, J. S. Moghaddas, and M. M. Ahadian, *Sci. Iran*, **17**, 122 (2010).
2. A. C. Pierre and G. M. Pajonk, *Chem. Rev.*, **102**, 4243 (2002).
3. C. A. M. Mulder and J. G. Lierop, "Preparation, Densification and Characterization of Autoclave Dried SiO_2 Gels", pp.68-75, Berlin, Germany, 1986.
4. L. W. Hrubesh, *Chem. Ind.*, **24**, 824 (1990).
5. S. Höffele, S. J. Russell, and D. B. Brook, *Int. Nonwoven. J.*, **14**, 10 (2005).
6. Z. Qi, D. Huang, S. He, H. Yang, Y. Hu, L. Li, and H. Zhang, *J. Eng. Fibre Fabr.*, **8**, 134 (2013).
7. A. Shaid, M. Fergusson, and L. Wang, *Chem. Mater. Eng.*, **2**, 37 (2014).
8. G. Rosace, E. Guido, C. Colleoni, and G. Barigozzi, *Int. J. Polym. Sci.*, Article ID 1726475 (2016).
9. M. Venkataraman, R. Mishra, J. Militky, and L. Hes, *Fiber. Polym.*, **15**, 1444 (2014).
10. M. Venkataraman, R. Mishra, T. M. Kotresh, T. Sakoi, and J. Militky, *J. Text. Inst.*, **107**, 1150 (2015).
11. M. Venkataraman, R. Mishra, J. Militky, and B. K. Behera, *J. Text. Inst.*, **108**, 1442 (2016).
12. X. Xiong, T. Yang, R. Mishra, and J. Militky, *Fiber. Polym.*, **17**, 1709 (2016).
13. T. Yang, X. Xiong, R. Mishra, J. Novák, and J. Militký, *Text. Res. J.*, doi:4051751668195 (2016).
14. M. Ghorannevissa, S. Shahidia, and B. Moazzenchia, *Surf. Coat. Tech.*, **201**, 4926 (2007).
15. G. Yuan, S. Jiang, E. Newton, J. Fan, and W. Au, *J. Text. Inst.*, **103**, 48 (2012).
16. J. Dembickỳ, *Fibre. Text. East. Eur.*, **18**, 80 (2010).
17. K. Singha, *Am. J. Polym. Sci.*, **2**, 39 (2012).
18. M. Stančić, D. Grujić, D. Novaković, N. Kašiković, B. Ružičić, and J. Geršak, *J. Graph. Eng. Des.*, **5**, 25 (2014).
19. A. M. Schneider and B. V. Holcombe, *Text. Res. J.*, **61**, 488 (1991).
20. M. V. Vivekanadan, S. Raj, S. Sreenivasan, and R. P. Nachane, *Indian J. Fiber Text.*, **36**, 117 (2011).
21. Y. K. Akimov, *Instrum. Exp. Tech+.*, **46**, 287 (2003).